ISSN 1674-1056
http://cpb.iphy.ac.cn
http://iopscience.iop.org/cpb
中国物理 B
Chinese Physics
中国物理
Chinese Physics B

# General analytical method of designing shielded coils for arbitrary axial magnetic field

Yi Zhang(张燚)[1], Yu-Jiao Li(李玉姣)[2], Qi-Yuan Jiang(江奇渊)[1], Zhi-Guo Wang(汪之国)[1], Tao Xia(夏涛)[1], Hui Luo(罗晖)[1]
**Citation:**Chin. Phys. B . 2019, 28(11): 110702 . **doi:** 10.1088/1674-1056/ab4d40
Journal homepage: http://cpb.iphy.ac.cn; http://iopscience.iop.org/cpb

**What follows is a list of articles you may be interested in**

---

## Optimization of pick-up coils for weakly damped SQUID gradiometers

Kang Yang(杨康), Jialei Wang(王佳磊), Xiangyan Kong(孔祥燕), Ruihu Yang(杨瑞虎), Hua Chen(陈桦)
Chin. Phys. B . 2018, 27(5): 050701 . **doi:** 10.1088/1674-1056/27/5/050701

## Performance study of aluminum shielded room for ultra-low-field magnetic resonance imaging based on SQUID: Simulations and experiments

Bo Li(李波), Hui Dong(董慧), Xiao-Lei Huang(黄小磊), Yang Qiu(邱阳), Quan Tao(陶泉), Jian-Ming Zhu(朱建明)
Chin. Phys. B . 2018, 27(2): 020701 . **doi:** 10.1088/1674-1056/27/2/020701

## Optical pumping nuclear magnetic resonance system rotating in a plane parallel to the quantization axis

Zhi-Chao Ding(丁志超), Jie Yuan(袁杰), Hui Luo(罗晖), Xing-Wu Long(龙兴武)
Chin. Phys. B . 2017, 26(11): 113301 . **doi:** 10.1088/1674-1056/26/11/113301

## Optical pumping nuclear magnetic resonance system rotating in a plane parallel to the quantization axis

Zhi-Chao Ding(丁志超), Jie Yuan(袁杰), Hui Luo(罗晖), Xing-Wu Long(龙兴武)
Chin. Phys. B . 2017, 26(9): 093301 . **doi:** 10.1088/1674-1056/26/9/093301

---

# General analytical method of designing shielded coils for arbitrary axial magnetic field*

Yi Zhang(张燚)[1], Yu-Jiao Li(李玉姣)[2], Qi-Yuan Jiang(江奇渊)[1], Zhi-Guo Wang(汪之国)[1,†], Tao Xia(夏涛)[1], and Hui Luo(罗晖)[1,‡]

[1] College of Advanced Interdisciplinary Studies, National University of Defense Technology, Changsha 410073, China
[2] College of Liberal Arts and Sciences, National University of Defense Technology, Changsha 410073, China

(Received 28 July 2019; revised manuscript received 12 September 2019; published online 30 October 2019)

Magnetic coils for specific requirements are widely used in modern quantum physics. In this study, a general analytical method of designing the shielded coils for generating an arbitrary axial magnetic field is proposed. The theoretical formula for an axial magnetic field generated by a single shielded coil is obtained and used to construct specific coils. The structural parameters of these coils are determined by fitting the theoretical formula with their specific requirements. The feasibility of this method is proved by realizing four concrete kinds of coils: uniform magnetic field generating coils, gradient magnetic field generating coils, asymmetrical uniform magnetic field generating coils, and parabolic magnetic field generating coils. The correctness of these theoretical results is demonstrated by both the finite element simulations and the relevant experimental results. Furthermore, the application of this method is of great significance for developing the quantum physics and quantum devices in future.

**Keywords:** magnetic coils, analytical method, shielding, quantum device

**PACS:** 07.55.–w, 07.55.Db, 33.25.+k **DOI:** 10.1088/1674-1056/ab4d40

## 1. Introduction

With the rapid development of quantum technology, specific magnetic field coils are increasingly required in many applications,[1] such as atomic clock,[2,3] optical pumped magnetometer,[4–8] nuclear magnetic resonance gyro,[9,10] and magnetic trap.[11–15] Although many kinds of magnetic coils[14–23] have been invented for these applications respectively, there is still a lack of a common method to design these coils conveniently, or even to realize any required magnetic field systematically. Moreover, lots of these existing coils[18–23] neglect the influence of magnetic shield which is important for the application in weak magnetic field.[2,4,5] These deficiencies would inevitably impede the evolution of quantum technology.

So in this study, we propose a general analytical method of designing the shielded coils for generating any required axial magnetic field. The rest of this paper is organized as follows. In Section 2 the theoretical formula for the axial magnetic field of a single coil in shield is derived and our design method is described generally. In Section 3 four concrete examples are used to demonstrate the feasibility of this method and also some significant practical coil designs are implemented. In Section 4 these four kinds of coils are realized experimentally. Finally, in Section 5 some conclusions are drawn from this study.

## 2. Theory

Without loss of generality, we first consider a thin coil with current density $\rho$ inside a closed cylindrical magnetic shield as described in Fig. 1.

Due to symmetry, there is only one component of the vector potential $A_\phi(r,z)$, which is not equal to zero.[24] Based on the Green's function,[25] in this case where the current density $\rho$ and radius $a$ of the thin coil are constants,

$$\begin{aligned} A_\phi(r,z) &= \mu_0 \int G(r,z,r',z')\,\rho(r',z')\,r'\mathrm{d}r'\mathrm{d}z' \\ &= \mu_0\rho a \int_{c-d}^{c} G(r,z,a,z')\,\mathrm{d}z' \\ &= \mu_0\rho a \sum_{\substack{n=0\\ i=e,o}}^{\infty} \int_{c-d}^{c} u_n^{\mathrm{i}}(r<)\,v_n^{\mathrm{i}}(r>)\,Z_n^{\mathrm{i}}(z)\,Z_n^{\mathrm{i}}(z')\,\mathrm{d}z' \\ &= \mu_0\rho a \sum_{\substack{n=0\\ i=e,o}}^{\infty} \int_{c-d}^{c} u_n^{\mathrm{i}}(r)\,v_n^{\mathrm{i}}(a)\,Z_n^{\mathrm{i}}(z)\,Z_n^{\mathrm{i}}(z')\,\mathrm{d}z', \end{aligned} \quad (1)$$

where $r<(r>)$ is the smaller (greater) one between $r$ and $a$, and[25]

$$\begin{aligned} &u_0^{\mathrm{e}}(r) = r/\sqrt{2}, \\ &u_{n>0}^{\mathrm{i}}(r) = \mathrm{Bi}_1\left(K_n^{\mathrm{i}} r\right), \\ &v_0^{\mathrm{e}}(r) = 1/\left(r\sqrt{2}\right), \end{aligned}$$

*Project supported by the National Natural Science Foundation of China (Grant Nos. 61701515 and 61671458), the Postdoctoral Science Foundation, China (Grant No. 2017M613367), the Natural Science Foundation of Hunan Province, China (Grant No. 2018JJ3608), and the Research Project of National University of Defense Technology, China (Grant No. ZK170204).

†Corresponding author. E-mail: maxborn@163.com
‡Corresponding author. E-mail: luohui.luo@163.com

© 2019 Chinese Physical Society and IOP Publishing Ltd 

$$
\begin{aligned}
&v^{\mathrm{i}}_{n>0}(r)=\mathrm{Bk}_1\left(K^{\mathrm{i}}_n r\right)+\mathrm{Bk}_0\left(K^{\mathrm{i}}_n b\right)\mathrm{Bi}_1\left(K^{\mathrm{i}}_n r\right)/\mathrm{Bi}_0\left(K^{\mathrm{i}}_n b\right),\\
&Z^{\mathrm{o}}_0(z)=0,\\
&Z^{\mathrm{o}}_{n>0}(z)=\sin\left(K^{\mathrm{o}}_n z\right)/\sqrt{h},\\
&Z^{\mathrm{e}}_0(z)=1/\sqrt{2h},\\
&Z^{\mathrm{e}}_{n>0}(z)=\cos\left(K^{\mathrm{e}}_n z\right)/\sqrt{h}
\end{aligned}
\tag{2}
$$

with[25]

$$
\begin{cases}
K^{\mathrm{e}}_n=n\pi/h,\\
K^{\mathrm{o}}_n=(n-1/2)\,\pi/h,
\end{cases}
\tag{3}
$$

where Bi and Bk are the modified Bessel functions of the first kind and second kind. Note that with the help of the dimensional analysis and the comparison with the first equation in Ref. [25], the expression of $v^{\mathrm{e}}_0(r)$ is modified through $1/\left(\sqrt{2r}\right)\to 1/\left(r\sqrt{2}\right)$. Based on these formulae, after integration, the explicit expression of $A_\phi(r,z)$ can be obtained as

$$
\begin{aligned}
A_\phi(r,z) &= \mu_0\rho a\left\{\frac{rd}{4ah}+\sum_{n=1}^{\infty}\int_{c-d}^{c}\right.\\
&\times\left[\frac{u^{\mathrm{e}}_n(r)\,\upsilon^{\mathrm{e}}_n(a)\cos\left(K^{\mathrm{e}}_n z\right)\cos\left(K^{\mathrm{e}}_n z'\right)}{h}\right.\\
&\left.\left.+\frac{u^{\mathrm{o}}_n(r)\,\upsilon^{\mathrm{o}}_n(a)\sin\left(K^{\mathrm{o}}_n z\right)\sin\left(K^{\mathrm{o}}_n z'\right)}{h}\right]\mathrm{d}z'\right\}\\
&= \mu_0\rho a\left[\frac{rd}{4ah}+\sum_{n=1}^{\infty}u^{\mathrm{e}}_n(r)\,\upsilon^{\mathrm{e}}_n(a)\cos\left(K^{\mathrm{e}}_n z\right)\right.\\
&\times\frac{\sin K^{\mathrm{e}}_n c-\sin K^{\mathrm{e}}_n(c-d)}{hK^{\mathrm{e}}_n}\\
&+\sum_{n=1}^{\infty}u^{\mathrm{o}}_n(r)\,\upsilon^{\mathrm{o}}_n(a)\sin\left(K^{\mathrm{o}}_n z\right)\\
&\left.\times\frac{\cos K^{\mathrm{o}}_n(c-d)-\cos K^{\mathrm{o}}_n c}{hK^{\mathrm{o}}_n}\right].
\end{aligned}
\tag{4}
$$

Since the corresponding axial magnetic field is given by[24]

$$
B_z(r,z)=\frac{1}{r}\frac{\partial\left[rA_\phi(r,z)\right]}{\partial r},
\tag{5}
$$

for the case in Fig. 1, the axial magnetic field generated by the single thin coil in shield can be described as

$$
\begin{aligned}
B_z(r,z,c) &= \mu_0\rho a\left\{\frac{d}{2ah}+\sum_{n=1}^{\infty}\mathrm{Bi}_0\left(K^{\mathrm{e}}_n r\right)\upsilon^{\mathrm{e}}_n(a)\cos\left(K^{\mathrm{e}}_n z\right)\right.\\
&\times\frac{\sin K^{\mathrm{e}}_n c-\sin K^{\mathrm{e}}_n(c-d)}{h}\\
&+\sum_{n=1}^{\infty}\mathrm{Bi}_0\left(K^{\mathrm{o}}_n r\right)\upsilon^{\mathrm{o}}_n(a)\sin\left(K^{\mathrm{o}}_n z\right)\\
&\left.\times\frac{\cos K^{\mathrm{o}}_n(c-d)-\cos K^{\mathrm{o}}_n c}{h}\right\}.
\end{aligned}
\tag{6}
$$

After substituting Eqs. (2) and (3) into Eq. (6), the final expression of the axial magnetic field is

$$
\begin{aligned}
&B_z(r,z,c)\\
&=\mu_0\rho\left\{\frac{d}{2h}+\frac{a}{h}\sum_{n=1}^{\infty}A_n(r)\cos\frac{n\pi z}{h}\right.\\
&\times\left[\sin\frac{n\pi c}{h}-\sin\frac{n\pi(c-d)}{h}\right]\\
&+\frac{a}{h}\sum_{n=1}^{\infty}A_{n-1/2}(r)\sin\frac{(n-1/2)\,\pi z}{h}\\
&\left.\times\left[\cos\frac{(n-1/2)\,\pi(c-d)}{h}-\cos\frac{(n-1/2)\,\pi c}{h}\right]\right\},
\end{aligned}
\tag{7}
$$

where

$$
\begin{aligned}
A_n(r) &= \mathrm{Bi}_0\left(\frac{n\pi r}{h}\right)\left[\mathrm{Bk}_1\left(\frac{n\pi a}{h}\right)\right.\\
&\left.+\mathrm{Bk}_0\left(\frac{n\pi b}{h}\right)\cdot\mathrm{Bi}_1\left(\frac{n\pi a}{h}\right)/\mathrm{Bi}_0\left(\frac{n\pi b}{h}\right)\right],
\end{aligned}
\tag{8}
$$

$a$, $c$, and $d$ are radius, axial position, and width of the coil, respectively, $b$ and $h$ are radius and half height of the magnetic shield as shown in Fig. 1(a). A concrete result of Eq. (7) is presented in Fig. 1(b), where $a=8$ mm, $c=8$ mm, $d=0.1$ mm, $b=9$ mm, $h=12$ mm, and $\rho=10^4$ A/m. It can be found that this result s accords well with that from the finite element calculation (see open circles), which can demonstrate the correctness of our derivation. In addition, it is worth mentioning that all the finite element calculation results in this study are obtained by using a widely used reliable simulation software named Maxwell 16.0.

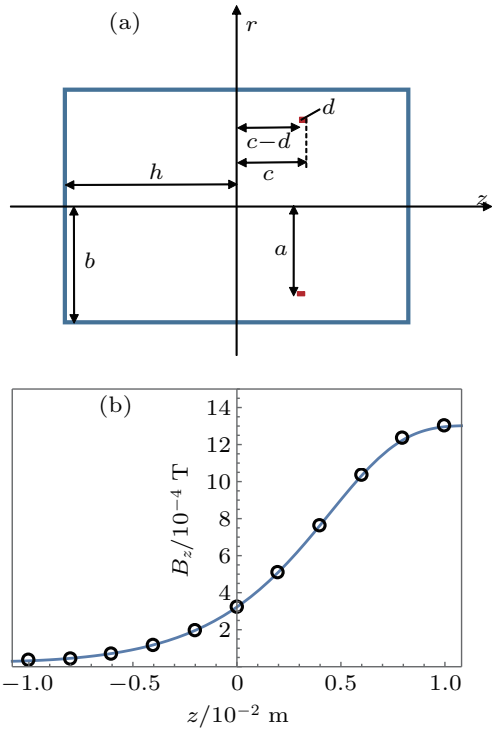



**Fig. 1.** (a) Single coil in shield and (b) its axial magnetic field where solid line represents results from Eq. (7) and empty circles denote results fromour finite element calculation.

As further simplifications, here we discuss symmetric double loop coils with parallel and anti-parallel currents, respectively. The figures are shown in Fig. 2

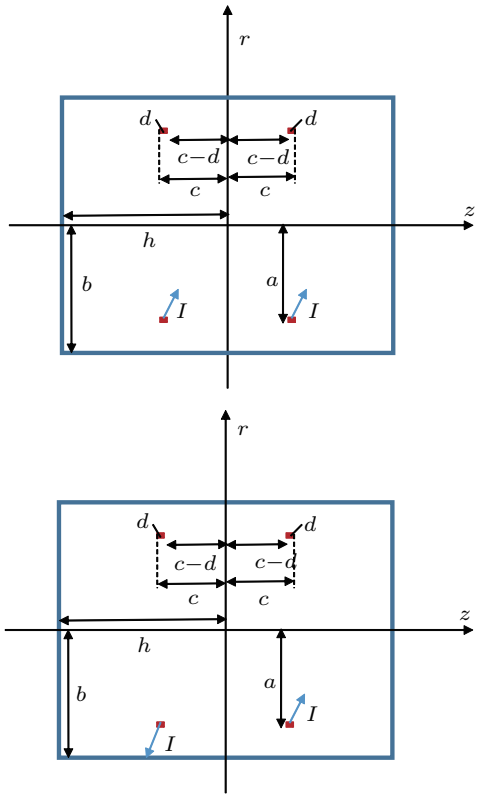



**Fig. 2.** Symmetric double loop coils with parallel and anti-parallel currents.

Based on Eq. (7), the magnetic field from symmetric double loop coils with parallel currents [as shown in Fig. 3(a)] is given by

$$\begin{aligned} B_z^{\mathrm{dp}}(r,z,c) &= B_z(r,z,c)+B_z(r,z,-c+d) \\ &= \mu_0\rho\left\{\frac{d}{h}+\frac{2a}{h}\sum_{n=1}^{\infty}A_n(r)\cos\frac{n\pi z}{h}\right. \\ &\quad \left.\times\left[\sin\frac{n\pi c}{h}-\sin\frac{n\pi(c-d)}{h}\right]\right\}. \end{aligned} \tag{9}$$

In the same way, the magnetic field from symmetric double loop coils with anti-parallel currents is

$$\begin{aligned} &B_z^{\mathrm{da}}(r,z,c) \\ &= B_z(r,z,c)-B_z(r,z,-c+d) \\ &= 2\mu_0\rho\left\{\frac{a}{h}\sum_{n=1}^{\infty}A_{n-1/2}(r)\sin\frac{(n-1/2)\pi z}{h}\right. \\ &\quad \left.\times\left[\cos\frac{(n-1/2)\pi(c-d)}{h}-\cos\frac{(n-1/2)\pi c}{h}\right]\right\}. \end{aligned} \tag{10}$$

The validity of Eqs. (9) and (10) can also be proved by comparing with the results from the finite element calculation, where the structural parameters are the same as those used in the single coil above.

So far, the key point of our general analytic design method is to utilize Eqs. (7), (9) or (10) to fit the specific magnetic requirements and to determine the coil structural parameters $a$, $c$, and $d$. Here for simplicity, we only take the axial position $c$ as a fitting variable. In fact, this is consistent with many practical situations,[18,19] where the radius $a$ and the width $d$ of the coil are fixed. In addition, when the fitting requirements are symmetric, equations (9) and (10) may be more effective with the same symmetry and this will be described below.

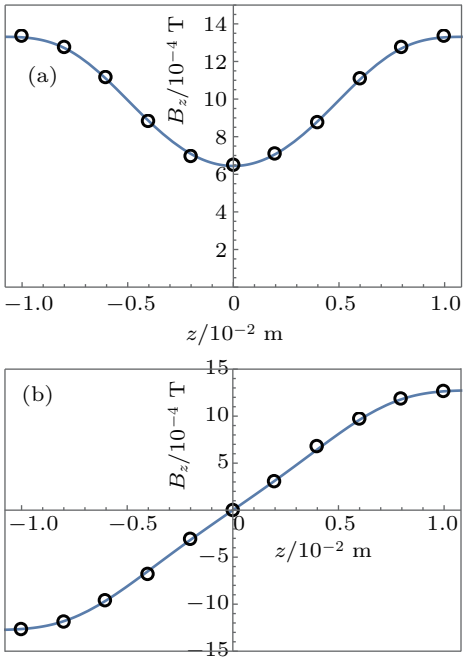



**Fig. 3.** Magnetic fields of symmetric double loop coils with parallel and anti-parallel currents.

## 3. Application and simulation

### 3.1. Uniform magnetic field coils

As the first practical application, here we use our design method to construct symmetric uniform magnetic field coils. Without loss of generality, we set the required axial magnetic field to be 0.1 T in the range $z\in[-h/2,h/2]$ as depicted by 21 solid triangles in Fig. 4.

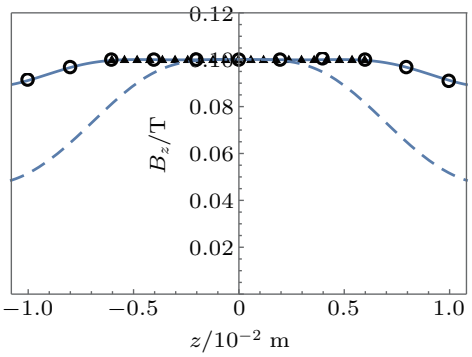



**Fig. 4.** Magnetic fields from our uniform coils and existing Helmholtz coils.

Due to the symmetry of this requirement, we use $B_z^{\mathrm{dp}}(r,z,c)$ to constitute an objective function

$$\begin{aligned} &B_z^{\mathrm{o}}(r,z,c_1,c_2,c_3) \\ &= B_z^{\mathrm{dp}}(r,z,c_1)+B_z^{\mathrm{dp}}(r,z,c_2)+B_z^{\mathrm{dp}}(r,z,c_3). \end{aligned} \tag{11}$$

After fitting, the structure parameters and current density can be determined to be $c_1 = 1.7$ mm, $c_2 = 6.8$ mm, $c_3 = 8$ mm, and $\rho = 3.0865 \times 10^6$ A/m. Other parameters not mentioned here are the same as those in Fig. 1. This result is shown by the solid curve and demonstrated by the empty circles from finite element calculation in Fig. 4. In addition, the dashed curve refers to the magnetic field from corresponding Helmholtz coils each with radius $a = 8$ mm, axial position $c = a/2 = 4$ mm, and parallel current density $\rho = 7.4077 \times 10^6$ A/m in the center of the shield. It can be seen that both the inhomogeneity $\delta B_z = \max\left|\left[B_z(z) - B_z(0)\right]/B_z(0)\right| = 0.0038$ and the uniform range $[-6\text{ mm}, 6\text{ mm}]$ of our coils are better than those of common Helmholtz coils (0.0050 and $[-2\text{ mm}, 2\text{ mm}]$).

### 3.2. Gradient magnetic field coils

As another usual application, we design gradient magnetic field coils through our method. The requirement for this case is that the axial magnetic field linearly changes from -0.006 T to 0.006 T in $z \in [-6\text{ mm}, 6\text{ mm}]$ as depicted by 21 solid triangles in Fig. 5.

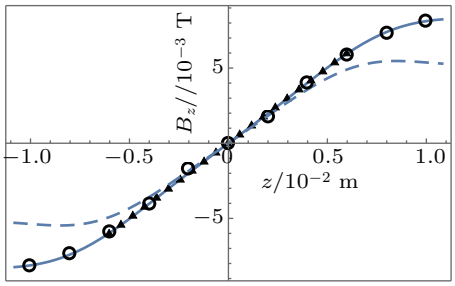



**Fig. 5.** Magnetic fields from our gradient coils and reverse Helmholtz coils.

Because of anti-symmetry of magnetic field, the objective function can be built by $B_z^{\mathrm{da}}(r,z,c)$ and expressed as follows:

$$\begin{aligned} &B_z^{\mathrm{o}}(r,z,c_1,c_2,c_3) \\ &= B_z^{\mathrm{da}}(r,z,c_1) + B_z^{\mathrm{da}}(r,z,c_2) + B_z^{\mathrm{da}}(r,z,c_3). \end{aligned} \tag{12}$$

After fitting, its parameters can be obtained to be $c_1 = 6.6$ mm, $c_2 = 8.4$ mm, $c_3 = 9.5$ mm, and $\rho = 2.1133 \times 10^5$ A/m. From Fig. 5, it can be found that the linearity and linear region of our coils are better than those of the reverse Helmholtz coils in shield with its radius $a = 8$ mm, axial position $c = a\sqrt{3}/2 \approx 6.9$ mm and anti-parallel current density $\rho = 5.0719 \times 10^5$ A/m which can eliminate the first nonlinear expansion term of its axial magnetic field. Similarly, the results (empty circles) from finite element calculation ensure the validity of our analytic formulae.

### 3.3. Asymmetrical uniform magnetic field coils

So far, we have discussed two kinds of symmetrical and anti-symmetrical coils described with Eqs. (9) and (10), respectively. With the help of Eq. (7) we investigate a more general case, named asymmetrical uniform magnetic field coils, whose center is not the center of the magnetic shield. This may be of great significance for miniaturizing the modern quantum devices and implementing other specific applications. The requirement for this case is that the axial magnetic field is 0.05 T in the range $z \in [3\text{ mm}, 9\text{ mm}]$ as depicted by 21 solid triangles in Fig. 6.

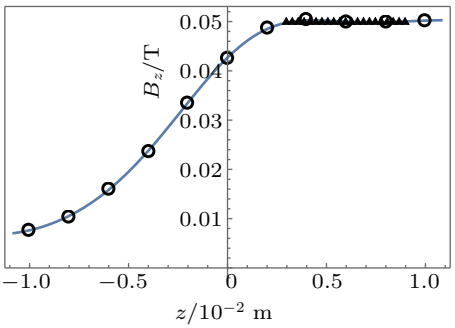



**Fig. 6.** Magnetic fields from asymmetrical uniform magnetic field coils.

This objective function for this asymmetrical case can be constructed by the general formula Eq. (7) as follows:

$$\begin{aligned} &B_z^{\mathrm{o}}(r,z,c_1,c_2,c_3) \\ &= B_z(r,z,c_1) + B_z(r,z,c_2) + B_z(r,z,c_3). \end{aligned} \tag{13}$$

Its fitting parameters can be obtained to be $c_1 = 0.2$ mm, $c_2 = 3.3$ mm, $c_3 = 9.5$ mm, and $\rho = 2.1823 \times 10^6$ A/m, which means that the coils and the uniform range are only on the right hand side of the shield as we expect. After the careful calculation, it can be found that the inhomogeneity $\delta B_z$ of our asymmetrical coils in the range $z \in [3\text{ mm}, 9\text{ mm}]$ is only 0.006, which can meet most practical requirement for uniform magnetic field. Similarly, the results from the finite element calculation (denoted by the empty circules) ensure the validity of our analytic formulae.

### 3.4. Parabolic magnetic field coils

Finally, for a more general case, we use our method to design the parabolic magnetic field coils, which may be used as a magnetic trap without Majorana loss.[14] In this case, as shown in Fig. 7, the requirement is depicted by 21 uniformly distributed solid triangles in the range $z \in [-6\text{ mm}, 6\text{ mm}]$, which satisfies the equation $B_z(z) = 1000z^2 + 0.03\,(T)$.

The objective function for this case is given by

$$\begin{aligned} &B_z^{\mathrm{o}}(r,z,c_1,c_2,c_3) \\ &= B_z(r,z,c_1) + B_z(r,z,c_2) + B_z(r,z,c_3) + B_z(r,z,c_4). \end{aligned} \tag{14}$$

The fitting parameters are $c_1 = -10.7$ mm, $c_2 = -10.4$ mm, $c_3 = 10.5$ mm, $c_4 = 10.8$ mm, and $\rho = 3.4144 \times 10^6$ A/m. It can be seen that the magnetic field generated by these parameters accords very well with the parabolic requirement and the results from the finite element calculation (denoted by empty

circles) prove this result. In fact, our method can be used to design the coils satisfying many different kinds of magnetic requirements, not limited to only these cases as mentioned above: this is why we use the word "arbitrary" in the title of this study.

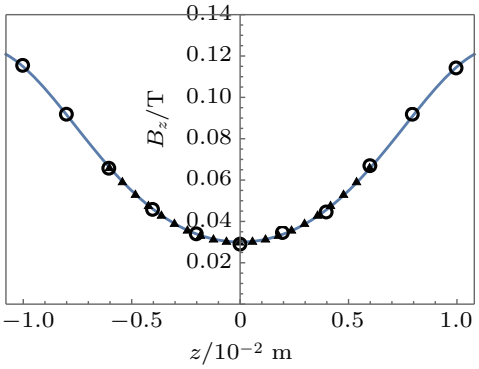



**Fig. 7.** Magnetic fields from parabolic magnetic field coils.

## 4. Experiment and discussion

In order to further demonstrate the feasibility of our approach and to conveniently measure the magnetic field, we design relevant experiments in a large-scaled system with $a = 191.0$ mm, $b = 218.0$ mm, $h = 366.5$ mm, $d = 3.0$ mm as described in Fig. 8. The white coils are assembled on the green calibrated slide rails, so that their positions can be flexibly adjusted to different parameters $\{c_i\}$ we required. Then they are pushed into the black 5-layer magnetic shielding and connected to an RIGOL DP831A current source with 0.8-A (0.1 A×8 turns) stable current. A CTM-6W fluxgate magnetometer is used to measure the magnetic field along the symmetry axis.

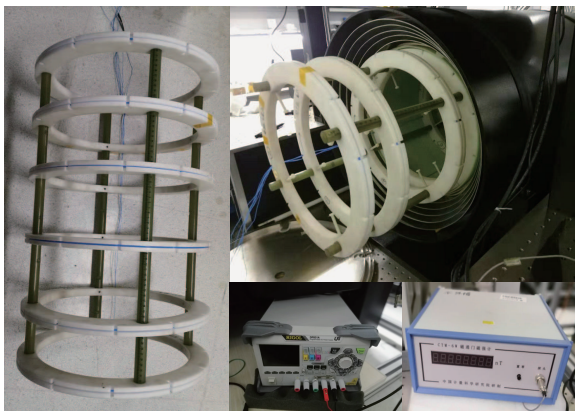


**Fig. 8.** Experimental equipment of magnetic measurement for different kinds of coils.

Figure 9 shows the experimental results of the uniform magnetic field coils with the parameters $c_1 = 61.5$ mm, $c_2 = 183.5$ mm, and $c_3 = 297.5$ mm from our method. It can be seen that the experimental results (open circles) accord very well with the theoretical ones (solid curve), which can further demonstrate the correctness of our analytic formulae and field inhomogeneity in the 400.0-mm range of the center (less than $5.7\times10^{-3}$), which could meet most practical requirements.

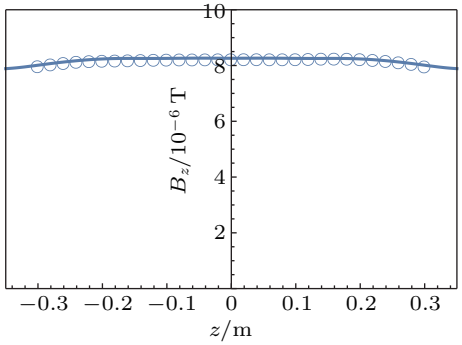



**Fig. 9.** Experimental and theoretical magnetic field of the uniform magnetic field coils.

Figure 10 displays the experimental results of the gradient magnetic field coils with the parameters $c_1 = 12.5$ mm, $c_2 = 205.5$ mm, and $c_3 = 262.0$ mm from our method. The experimental results (open circles) are also in accordance with the theoretical ones (solid curve) in the central functional area.

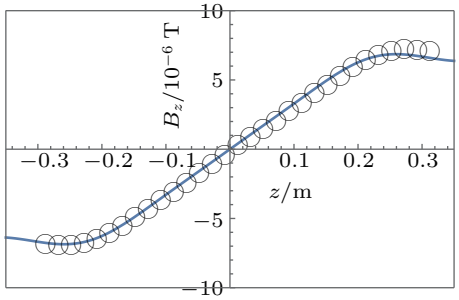



**Fig. 10.** Experimental and theoretical magnetic field of gradient magnetic field coils.

The experimental (empty circles) and theoretical (solid curve) results of the asymmetrical uniform magnetic field coils with the parameters $c_1 = 6.0$ mm, $c_2 = 131.0$ mm, and $c_3 = 292.0$ mm from our method are shown in Fig. 11. The inhomogeneity of the 180.0-mm uniform range on the right side is below $8.4\times10^{-3}$, which could be used in some specific magnetic systems.

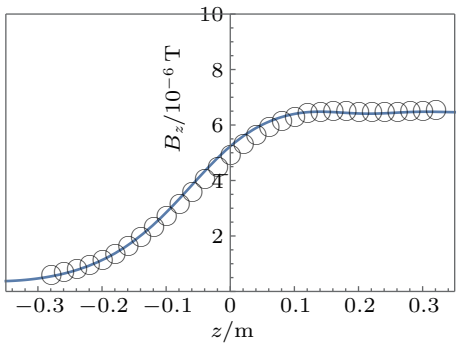



**Fig. 11.** Experimental and theoretical magnetic field of asymmetrical uniform magnetic field coils.

Finally, figure 12 shows that the experimental results (open circles) and the theoretical (solid curve) results of

the parabolic magnetic field coils with the parameters $c_1 = -308.5$ mm, $c_2 = -228.5$ mm, $c_3 = 231.5$ mm, and $c_4 = 311.5$ mm from our method, and they accord very well with each other.

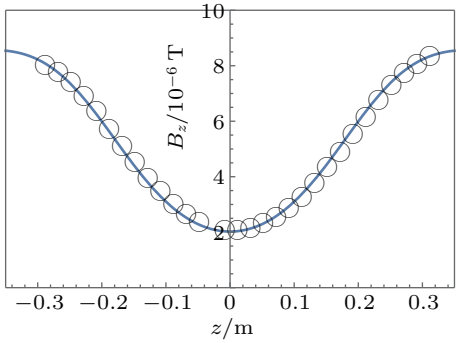



**Fig. 12.** Experimental and theoretical magnetic field of parabolic magnetic field coils.

## 5. Conclusions

In this work, a general analytical method of designing the shielded coils for generating an arbitrary axial magnetic field is proposed. The basic theoretical formulae [Eqs. (7), (9), and (10)] for axial magnetic field in shield are obtained and used to construct four common kinds of coils: coils for generating a uniform magnetic field, coils for a gradient magnetic field, coils for an asymmetrical uniform magnetic field, and coils for a parabolic magnetic field. The structural parameters of these coils are determined by fitting the formulae with their specific requirements. Results prove the feasibility of this method and show some advantages of these coils. For example, both the uniformity and the uniform range of the uniform magnetic field coils are better than those in the existing Helmholtz coils. Finally, all these results accord well with those from both the finite element simulations and relevant experiments, thus demonstrating the correctness of our formulae in this study.

## References

[1] Li Y Y, Wang Z N and Wang S S 2017 *Physics* **46** 307 (in Chinese)
[2] Yano Y, Goka S and Kajita M 2017 *Appl. Phys. B* **123** 67
[3] Zhao F J, Gao F, Han J X, Zhou C H, Meng J W, Wang Y B, Guo Y, Zhang S G and Chang H 2018 *Acta Phys. Sin.* **67** 050601 (in Chinese)
[4] Zhou F, Zhu C J, Hagley E W and Deng L 2017 *Sci. Adv.* **3** e1700422
[5] Zhao B B, Guo H, Zhao R, Du F F, Li Z H, Wang L, Wu D J, Chen Y L, Tang J and Liu J 2016 *IEEE Magn. Lett.* **7** 1
[6] Li S G, Zhou X, Cao X C, Sheng J T, Xu Y F, Wang Z Y and Lin Q 2010 *Acta Phys. Sin.* **59** 877 (in Chinese)
[7] Fang J C, Wang T, Zhang H, Li Y and Cai H W 2015 *Chin. Phys. B* **24** 060702
[8] Li R J, Quan W, Fan W F, Xing L, Wang Z, Zhai Y Y and Fang J C 2017 *Chin. Phys. B* **26** 120702
[9] Meyer D and Larsen M 2014 *Gyroscopy & Navigation* **5** 75
[10] Chen L L, Zhou B Q, Lei G Q, Wu W F, Zhai Y Y, Wang Z and Fang J C 2017 *AIP Adv.* **7** 115101
[11] Pritchard D E 1983 *Phys. Rev. Lett.* **51** 1336
[12] Migdall A L, Prodan J V, Phillips W D, Bergeman T H and Metcalf H J 1985 *Phys. Rev. Lett.* **54** 2596
[13] Soding J, Guery-Odelin D, Desbiolles P, Ferrari G and Dalibard J 1998 *Phys. Rev. Lett.* **80** 1869
[14] Esslinger T, Bloch I and Hansch T W 1998 *Phys. Rev. A* **58** R2664
[15] Paul W 1990 *Angew. Chem. Int. Edit.* **29** 739
[16] Wang Y H, Liu F, Li Y, Tang F F and Crozier S 2016 *J. Magn. Reson.* **269** 203
[17] While P T, Korvink J G and Shah N J 2013 *J. Magn. Reson.* **235** 85
[18] Abbott J J 2015 *Rev. Sci. Instrum.* **86** 054701
[19] Beiranv R 2014 *Rev. Sci. Instrum.* **85** 055115
[20] Knopp T, Sattel T F and Buzug T M 2012 *IEEE Magn. Lett.* **3** 6500104
[21] Sasada I and Nakashima Y 2006 *J. Appl. Phys.* **99** 08D904
[22] Wang J, She S and Zhang S 2002 *College Physics* **73** 2175
[23] Koss P A, Crawford C, Bison G, Wursten E, Kasprzak M and Severijns N 2017 *IEEE Magn. Lett.* **8** 1306205
[24] Hanson R J and Pipkin F M 1965 *Rev. Sci. Instrum.* **36** 179
[25] Robert H L and Chauncey U 1975 *Rev. Sci. Instrum.* **46** 337